Transition radiation in metal-metal multilayer nanostructures as a medical source of hard x-ray radiation

A. L. Pokrovsky and A. E. Kaplan[a)]
Electrical and Computer Engineering Department, The Johns Hopkins University, Baltimore, Maryland 21218

P. L. Shkolnikov
Electrical and Computer Engineering Department, State University of New York at Stony Brook, Stony Brook, New York 11794

(Received 9 February 2006; accepted 20 July 2006; published online 31 August 2006)

We show that a periodic metal-metal multilayer nanostructure can serve as an efficient source of hard x-ray transition radiation. Our research effort is aimed at developing an x-ray source for medical applications, which is based on using low-energy relativistic electrons. The approach toward choosing radiator-spacer couples for the generation of hard x-ray resonant transition radiation by few-MeV electrons traversing solid multilayer structures for the energies of interest to medicine (30–50 keV) changes dramatically compared with that for soft x-ray radiation. We show that one of the main factors in achieving the required resonant line is the *absence of the contrast* of the refractive indices between the spacer and the radiator *at the far wings* of the radiation line; for that purpose, the optimal spacer, as a rule, should have a higher atomic number than the radiator. Having experimental goals in mind, we have considered also the unwanted effects due to bremsstrahlung radiation, absorption and scattering of radiated photons, detector-related issues, and inhibited coherence of transition radiation due to random deviation of spacing between the layers. Choosing as a model example a Mo–Ag radiator-spacer pair of materials, we demonstrate that the x-ray transition radiation line can be well resolved with the use of spatial and frequency filtering.
 [DOI: 10.1063/1.2335974]

I. INTRODUCTION

One of the promising medical applications of hard x rays is a so called bichromatic x-ray contrast diagnostics[1,2] whereby the absorption edge of a dye of interest (e.g., iodine) is "bracketed" by two (usually very broad) bands of radiation. The x-ray source for that application explored so far was synchrotron radiation of a large accelerator,[3] which makes it impractical for wider use. To make it compact and practical, one needs to develop an x-ray source with narrow radiation lines of sufficient photon flux and much lower electron accelerator energy.[4] An ideal way to go would be to employ the narrow-line resonant transition radiation (TR) of electrons traversing a multilayer solid-state nanostructure, proposed in Ref. 5. Since the main domain of interest are hard x rays beyond, e.g., 20 keV, the only effect that may provide any noticeable contrast of refractive index between the nanostructure layers is the narrow-line change of the refractive index in the close vicinity of absorption lines (so called atomic edges) of *K*, *L*, or *M* shells of one of the alternating layer elements (the so called *radiator*[5] alternated by nonresonant *spacers*).

Our research effort is aimed at developing an x-ray source that would rely on the use of low-energy electrons, and it is based on the earlier work[5] of two of us, which has theoretically demonstrated feasibility of generating intense x-ray transition radiation by few-MeV electrons traversing solid multilayer nanostructures. Generation of soft x rays via resonant TR in a multilayer submicron structure, albeit without the use of the dielectric contrast near the atomic photoabsorption edges, has been experimentally demonstrated in Ref. 6. The most dramatic difference of the results[5,6] (see also Ref. 7) from the main body of works on x-ray TR (Ref. 8) (see also references in Ref. 5) is the possibility to use electron (E) beams of 5–10 MeV energy to generate x rays in 30–50 keV range, whereas the conventional technology, based on foil stacks, needs electron energies three to four orders of magnitude higher. As a result, widely available and relatively inexpensive industrial and medical electron accelerators could be used instead of electron synchrotrons of the national-facility kind, and thus, low-cost sources of x rays for numerous practical applications can be developed. Another method we employ, also based on results,[5] is the utilization of resonances at inner-shell absorption edges of materials to narrow the bandwidth of the generated radiation and greatly enhance the intensity of the TR at each interface due to relatively large contrast of dielectric constants of the adjacent layers based on the huge jumps of absorption in the spectral vicinity to the inner-shell absorption edges.

The paper is organized as follows: In Sec. II we discuss the problem of choosing the radiator-spacer pairs. We formulate the requirements on the material parameters and compare with those for the materials suitable for generation of TR in the soft x-ray domain. Next, we provide expressions for calculation of the TR differential efficiency (Sec. III), based on which we choose specific pairs of materials and

[a)]Electronic mail: sasha@striky.ece.jhu.edu

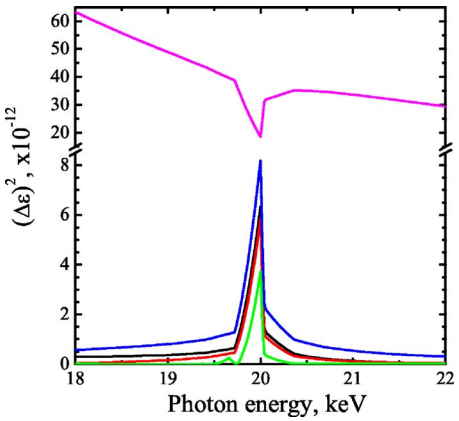

FIG. 1. (Color online) The contrast of dielectric constants $|\Delta\epsilon(\omega)|^2$ for Mo–Si, Mo–Tl, Mo–Ag, Mo–Pb, and Mo–Th (upper to lower curves, respectively).

study their radiation efficiency (Sec. IV). Comparison of the TR with the bremsstrahlung (BS) radiation, the main source of "noise" limiting efficiency of the metal-metal nanostructures as a source of hard x-ray TR, is provided in Sec. V. Section VI is devoted to discussing the measurement arrangement and detectors suitable for the proof-of-principle experiment we have planned. Then we discuss effects of the random layer width fluctuations (e.g., due to manufacturing inaccuracy) on the coherency of the TR; we also calculate precision tolerance of the nanostructure period allowing for substantial coherency gain in the output signal (Sec. VII).

II. SELECTION OF RADIATOR-SPACER PAIRS

The requirement of sufficiently hard x rays suggests relatively heavy atoms with respectively high K shells as the choice for a radiator. Currently, the most used element for a dye is *iodine*; recent research results[9] indicated that better results from the medical point of view can be achieved by using *Gadolinium*. Our preliminary search identified two "bracketing" radiator elements for iodine ($Z=53$, $E_K \approx 33\,169$ keV), Te ($Z=52$, $E_K \approx 31\,814$ keV) and Ba ($Z=56$, $E_K \approx 37\,441$ keV), and two "bracketing" radiator elements for gadolinium ($Z=64$, $E_K \approx 50\,239$ keV), Eu ($Z=63$, $E_K \approx 48\,519$ keV) and Tb ($Z=65$, $E_K \approx 51\,995$ keV).

Our original approach[5] aimed mostly at soft x-ray domain, and it was based on choosing the layer of heavy atoms as radiator with a chosen K-shell transition, and the layer of light atoms as a neutral spacer. However, in our detailed calculations we realized that approach while good for the soft x-ray domain does not produce desirable results in the hard x-ray domain. The major drawback is that in the 20–50 keV x-ray domain the TR spectrum with such pairs shows a spectral *dip* at the chosen K shell, instead of a desired spectral *peak* (see top curve in Fig. 1). While this effect may be beneficial for certain applications, in our case it proved to be counterproductive.

The problem on how to break through this obstacle by finding an approach to the proper choice of the radiator-spacer pairs arose. Our search through the periodic table of elements resulted in locating a few candidates of spacers for any given radiator to produce strongly pronounced resonant *peak* of transition radiation with the contrast better than two orders of magnitude. Surprisingly enough, these spacer candidates as a rule are *heavier* than the radiator. One of the requirements on the candidates we imposed is that they have to be technologically viable and accessible, which narrows down the field of candidates, but still leaves at least two candidates for each radiator element. The very major factor in the TR excited by electrons passing though a layered structure is that it occurs because of the difference (contrast), $\Delta\epsilon=\epsilon_s-\epsilon_r$,[10] between the dielectric constants of the adjacent layers at the frequency ω (or photon energy $E_{\rm ph}=\hbar\omega$) of radiation, where the subscripts s and r denote spacer and radiator, respectively. The energy of the TR at the frequency ω is proportional to $|\Delta\epsilon(\omega)|^2$. Here are the major requirements for the choice of materials.

- The radiator and spacer should have a largest possible $\Delta\epsilon$ between them at the central frequency of the radiation line. In the domain of interest, the atomic absorption edges are due to K-shell ionization, and the radiator should comprise relatively heavy atoms, starting from Mo ($E_K=20$ keV).
- At the same time, the radiator and spacer should have a very close dielectric constants at the wings of the radiation line, since otherwise, there will be a strong TR at the far wings, and the peak of radiation at the K-shell frequency will be very indistinct and of no use for the application in consideration.

Essentially, this is a signal-to-noise ratio problem; we should be seeking for the couples with $|\Delta\epsilon_{\rm wings}|^2 \ll |\Delta\epsilon_{\rm center}|^2$. This *wing-matching* condition immediately narrows down our options to both the spacer and radiator comprising *heavy* atoms, or more precisely, having high nuclei Coulomb charge Z. The latter condition is based on the following considerations. The lightest atom in the desirable domain is Mo, with nuclei Coulomb charge, and thus total number of electrons in a neutral atom, being $Z=42$.

The rest of the atoms in that domain have even higher Z. In the frequency domain of interest the dielectric constant of material could be written as $\epsilon \approx 1-2\delta$, with $0<\delta \ll 1$. Away from the K atomic absorption edge of the radiator yet reasonably close to it (within a few percents of the frequency), we have $\delta \propto f_1$ with $f_1 \sim Z$, where $0<Z-f_1 \ll Z$ and f_1 is the real part of the so called scattering factor.[5] At the very edge of the atomic K resonance, the largest possible deviation of f_1 from Z would be about $\ln(\Gamma_K)$ where Γ_K is the natural (i.e., due to radiation) dumping factor, and it is getting larger for heavier atoms. Thus, the largest difference $Z-f_1 \sim \ln(\Gamma_K)$ would be around 9 (in real terms it is usually lower than 8), with the relative contrast being $\sim$20% or even lower for heavier atoms.

If one chooses now a spacer with much lighter atoms, its dielectric constant would be determined by $\delta_s \propto Z_s$, where $Z_s \ll Z_r$ is the total number of atomic electrons for the spacer atoms [for high frequencies near the atomic edge of a heavy radiator, we have $(f_1)_s=Z_s$]. Thus, the difference $\Delta\epsilon=2(\delta_r-\delta_s)$ will be almost fully determined by the heavy atoms of the radiator, with the spacer having very little impact, since $\delta_r-\delta_s \ll \delta_r$ and thus $\Delta\epsilon \approx 2\delta_r$. Of course, δ depends also on

the atomic density, but taking it into consideration does not change the matter significantly; in most of the cases it only further diminishes the contribution of the spacer atoms. Therefore, for all the practical purposes, the system with light spacer+heavy radiator would behave almost like vacuum+radiator, so that at the wings there will be strong background radiation with its intensity proportional to Z_r^2, whereas at the atomic absorption edge of the radiator, it will be proportional to $(Z_r - |\ln \Gamma_r|)^2$, i.e., there will be a dip in the spectrum of radiation, rather than a resonant peak. As an example, we considered the technologically simplest pair, Mo–Si, which is well researched and made to order as extreme ultraviolet (EUV) mirrors: TR spectrum for such a pair would exhibit a dip near E_K of Mo (see upper curve in Fig. 1).

This explains why the "light spacer+heavy radiator" idea, good for the soft x-ray domain, fails to deliver an expected resonant line for the applications we are aiming at. Thus, for the hard x-ray domain one has to use the couples with the spacer being also a heavy element having Z_s fairly close to Z_r, so that the "wing-match" condition would be satisfied and, therefore, the radiation at the wings would be quenched by having almost vanishing $\Delta\epsilon$. The rule of thumb for the acceptable formula becomes "heavy radiator +heavier spacer."

III. TRANSITION RADIATION EFFICIENCY OF A MULTILAYER STRUCTURE

Spatial intensity distribution of resonant TR is conical, with most of the intensity at each particular wavelength λ concentrating about a certain emission angle θ measured from the electron velocity. Each TR spatial mode with a number r has a different resonant angle θ_r related to the wavelength and to the electron velocity v by the resonant condition

$$\overline{\epsilon^{1/2}} \cos\theta_r = \frac{c}{v} - \frac{r\lambda}{l}, \tag{1}$$

where $\overline{\epsilon^{1/2}} = (\sqrt{\epsilon_1} l_1 + \sqrt{\epsilon_2} l_2)/l$ is the mean refractive index of the medium, l_1 and l_2 are the thicknesses of different individual layers, $l = l_1 + l_2$ is the spatial period, and c is the velocity of light in vacuum. Equation (1) provides the condition for a constructive coherent interference of electromagnetic waves generated at different interfaces, at a distant point. Transition radiation differential efficiency in a multilayer structure, defined as the number of photons N per electron per unit solid angle Ω per unit interval of the TR frequency, can be expressed as[5,11–14]

$$\frac{d^2N}{d\Omega d\omega} = F_1 F_2 F_3, \tag{2}$$

where F_1 is the differential efficiency of a single interface, F_2 reflects the contribution of a single plate (i.e., of the very first couple of adjacent interfaces), and F_3 represents coherent summation of radiation from all the periods (i.e., couples of individual adjacent layers). For a strongly relativistic beam, i.e., when $\beta = v/c \approx 1$ and the relativistic factor $\gamma = (1 - \beta^2)^{-1/2}$ is high, $\gamma^2 \gg 1$, the differential efficiency of a single interface is

$$F_1 = \frac{\alpha(\Delta\epsilon)^2}{\pi^2\omega}|G|^2, \tag{3}$$

where $\Delta\epsilon = \epsilon_1 - \epsilon_2$ is the difference between the dielectric constants of the structure layers, $\alpha = 1/137$ is the fine structure constant, and G is a radiation pattern of a single interface given by

$$G \approx -\frac{\theta}{(\gamma^{-2} + \theta^2)^2}, \quad \theta \ll 1, \tag{4}$$

so that the angle of maximum radiation is $\theta_{\max\,\mathrm{rad}} \approx 1/(\gamma\sqrt{3})$.

The factor F_2 in Eq. (2) is due to coherent summation of radiation generated at the very first couple of adjacent interfaces. If we choose an angle of radiation, $\theta \approx \gamma^{-1}$, optimized for the *first* mode, $r = 1$, then we have for the rth resonance

$$F_2 = 4\sin^2\left[\frac{\pi(1 + \gamma^2\theta_r^2)}{4}\right]. \tag{5}$$

Note that working far below the Cherenkov radiation, i.e., if either $\epsilon < 1$ or $\epsilon - 1 \ll \gamma^{-2}$, which is always the case in our situation, the condition of the rth resonance [derived from Eq. (1)],

$$\theta_r^2 + \gamma^{-2} = \frac{2r\lambda}{l}, \quad l = \lambda\gamma^2, \tag{6}$$

gives

$$\theta_r^2 = \frac{(2r-1)}{\gamma^2} = \theta_1^2(2r-1), \tag{7}$$

so that $F_2 = 4\sin^2(r\pi/4)$, i.e.,

$$F_2 = 4 \quad \text{for } r = 1,3,\ldots \text{ and } F_2 = 0 \quad \text{for } r = 0,2,4,\ldots . \tag{8}$$

Thus, the even modes r are suppressed; be reminded that this is due to fact that at each neighboring interface the TR waves have different signs, since $\Delta\epsilon$ changes its sign at each successive interface.

Finally, for a single electron traversing M periods, each period consisting of two adjacent layers of alternating *lossless* materials, the multilayer factor F_3 for coherent summation of TR from each period is

$$F_3 = \frac{\sin^2(MX)}{\sin^2(X)}, \tag{9}$$

where X is a half-phase difference between each period; in our case

$$X \approx \frac{l\pi(\gamma^{-2} + \theta^2)}{2\lambda} \approx \frac{\pi(1 + \gamma^2\theta^2)}{2}. \tag{10}$$

The factor F_3 exhibits the resonances at the modes r occurring at $X_r = r\pi$. Since the number of periods should be high, $M \gg 1$, the radiation pattern of the multilayer structure will be concentrated very nearly the rth resonant angle

$$\theta_r = \gamma^{-1}\sqrt{2r-1}, \tag{11}$$

so that in the close vicinity of each resonance, $\theta=\theta_r+\Delta\theta$, with $\Delta\theta \ll \theta_r \ll 1$, we can write

$$X_r \approx r\pi + \pi\gamma\sqrt{2r-1}\Delta\theta \tag{12}$$

and

$$(F_3)_r \approx \frac{sin^2(M\pi\gamma\sqrt{2r-1}\Delta\theta)}{(\pi\gamma\sqrt{2r-1}\Delta\theta)^2}, \quad r=1,3,5,\ldots . \tag{13}$$

Notice that in the case of exact resonance, $X=0$, or $\Delta\theta=0$, we can write (9) and (13) in the form

$$F_3 = M^2. \tag{14}$$

According to Eq. (4) we can write now

$$\frac{d^2N_r}{d\Omega d\omega} = \frac{\alpha(\Delta\epsilon)^2\gamma^6(2r-1)\sin^2(M\pi\gamma\sqrt{2r-1}\Delta\theta)}{4r^4\pi^2\omega(\pi\gamma\sqrt{2r-1}\Delta\theta)^2}. \tag{15}$$

Integrating over the solid angle, $d\Omega=2\pi\sin\theta d\theta \approx 2\pi\theta_r d(\Delta\theta)$, from $\Delta\theta=-\infty$ to $\Delta\theta=\infty$, and having in mind that $\int_{-\infty}^{\infty}\sin^2(x)/x^2dx=\pi$, we have the total number of photons generated in the rth mode at the frequency ω:

$$\frac{dN_r}{d\omega} = \frac{\alpha(\Delta\epsilon)^2}{\pi\omega}\frac{M\gamma^4(2r-1)}{2r^4}. \tag{16}$$

The total number of the photons in all the modes at the frequency ω is

$$N_\Sigma = \sum_{r=1}^{\infty} N_r \quad \text{with } r=2k-1. \tag{17}$$

From (16) we have

$$\frac{dN_1}{d\omega} = \frac{\alpha(\Delta\epsilon)^2}{2\pi\omega}M\gamma^4 \text{ and} \tag{18}$$

$$\frac{N_3}{N_1} \approx 0.0617, \quad \frac{N_5}{N_1} \approx 0.008,$$

$$\frac{N_7}{N_1} \approx 0.0054, \quad \frac{N_9}{N_1} \approx 0.0026, \ldots, \tag{19}$$

which shows that the main mode with $r=1$ carries $\sim$92% of the entire radiation, so the rest of the modes are insignificant. Anyway, summing up all the modes up to $r=101$, we find

$$\frac{dN_\Sigma}{d\omega} \approx 1.1M\gamma^4\frac{\alpha(\Delta\epsilon)^2}{2\pi\omega}. \tag{20}$$

Equation (20) can be modified to take the photoabsorption[10,15,16] into account as follows:

$$\frac{dN_\Sigma(\omega)}{d\omega} \approx \frac{1.1\gamma^4\alpha[\Delta\epsilon(\omega)]^2L_{\text{attn}}}{2\pi\omega l}(1-e^{-lM/L_{\text{attn}}}), \tag{21}$$

where $L_{\text{attn}}=2(L_1^{-1}+L_2^{-1})^{-1}$ is the mean attenuation length, with L_i being the attenuation lengths of the materials comprising the structure.[5]

As we show below, to measure the TR one should use spatial filtering. Thus, the experimental data would be better characterized not by the radiation efficiency integrated over all modes and all angles but rather by TR angular distribution in the vicinity of the first resonance. In this case, the TR differential efficiency with photoabsorption and electron scattering taken into account can be calculated using Eqs. (2)–(5) where instead of Eq. (13) for F_3 one should use $\tilde{F}_3$

$$\tilde{F}_3 = e^{-(M-1)(\xi+\rho)}\frac{\cosh[M(\xi-\rho)]-\cos(2MX)}{\cosh(\xi-\rho)-\cos(2X)}, \tag{22}$$

where $\xi=(\mu_1 l_1+\mu_2 l_2)/(2\cos\theta)$ is the mean photoabsorption coefficient of the structure, μ_i is the photoabsorption coefficient of the ith material, $i=1,2$, $\rho=l/(2L_{\text{cr}})$, $L_{\text{cr}}=[(dE/dz)_1(l_1/l)+(dE/dz)_2(l_2/l)]$ is a distance at which nearly all electrons become scattered or absorbed, and dE/dz are the electron-atom collision losses per unit length calculated as[5]

$$\left(\frac{dE}{dz}\right)_i = \frac{2\pi mc^2r_e^2Z_iN_{Ai}}{\beta^2}\left[\ln\frac{(\gamma-1)^2(\gamma+1)}{2I_i^2} + \frac{(\gamma-1)^2/8-(2\gamma-1)\ln 2+1}{\gamma^2}\right], \tag{23}$$

where m is the rest mass of the electron, $r_e=e^2/(mc^2)=2.82\times10^{-13}$ cm is the classical electron radius, e is the electron charge, $I_i=9.73Z_i+58.8Z_i^{-0.19}$ eV is the approximate ionization potential of the atom (for atomic number $Z_i>13$), and N_{Ai} are the atomic number densities.

IV. DESIGN OF EXPERIMENT

Aiming to design a proof-of-principle experiment, we have chosen as a radiator an element widely used in the x-ray technology (e.g., for x-ray and EUV mirrors), whose properties are well known and which is readily available, *molybdenum* ($Z=42$), and which has K shell at $E_K=19.9995$ keV. Next, we conducted a search of the spacer, which revealed a number of materials suitable for the Mo radiator. These materials are Pb, Ag, Tl, and Th, which provide a very convenient set of options; for instance, lead (Pb) as a spacer has a great advantage of being accessible and technologically easily manageable. Another advantage also is that lead has a great tolerance to mismatching of the crystal lattice constants (this mismatch usually creates problem with mechanical stability of multilayer structures). The contrast of dielectric constants, $|\Delta\epsilon(\omega)|^2$ for Mo–Pb, Mo–Ag, Mo–Tl, and Mo–Th pairs, shown in Fig. 1 demonstrates a well pronounced peak near E_K of Mo, and the wing-matching condition is clearly satisfied, which differs significantly from the light spacer +heavy radiator structures (e.g., Mo–Si, upper curve in Fig. 1).

Let us focus on the E-beam of 30 MeV energy[17] and calculate the transition radiation efficiency, integrated over all the angles and modes, using Eq. (21), which takes the photoabsorption into account. Note that the effects of electron scattering are negligible as compared to the photoabsorption for the TR structures and E-beams under study [$L_{\text{cr}} \gg L_{\text{attn}}$; see Eqs. (21) and (23)].

The TR spectra (Fig. 2) for the most efficient couples, Mo–Ag, Mo–Tl, and Mo–Pb, clearly demonstrate the

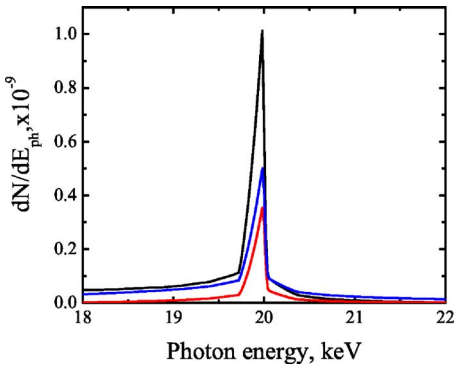

FIG. 2. (Color online) Transition radiation efficiency in number of photons per electron per 1 eV photon energy vs photon energy for 400-period Mo–Ag, Mo–Tl, and Mo–Pb (upper to lower curves, respectively) nanostructures with the period $l=0.2232$ μm. Electron energy is 30 MeV.

strongly pronounced resonant line, with contrast between the wings and the center easily reaching two orders of magnitude. The radiation lines shown in Fig. 2 have ~1% total linewidth. One can see that even though the peak value of $|\Delta\epsilon(\omega)|^2$ is largest for Mo–Tl structure (Fig. 1), with photoabsorption taken into consideration the most efficient couple of radiator and spacer is Mo–Ag (Fig. 2), which we focus at in the rest of our paper.

As the thickness of structure increases up to the attenuation length and beyond it, the photon output is getting saturated. In practical terms, it would be reasonable to keep up to ~1000 periods in Mo–Ag structure, as one can see in Fig. 3 that depicts the total number of generated TR photons within a resonant line versus the total thickness of the structure. The total number of photons per electron in the Mo–Ag nanostructure is about 3×10^{-7}.

It is easy to see that this efficiency is high enough for medical applications discussed in Sec. I. Indeed, using this structure with, e.g, a reconditioned medical accelerator Clinac (see, e.g., Ref. 18) at 30 MeV electron energy, 120 Hz repetition rate, and 2μs pulse duration, we arrive at 6×10^7 photons/s flux. This flux is essentially the same as the one utilized in the prototype bichromatic x-ray contrast diagnostics (see, e.g., Ref. 5); however, instead of a large synchrotron used in that prototype, TR from a Mo–Ag nanostructure involves a modest-size medical electron accelerator, affordable to any large hospital.

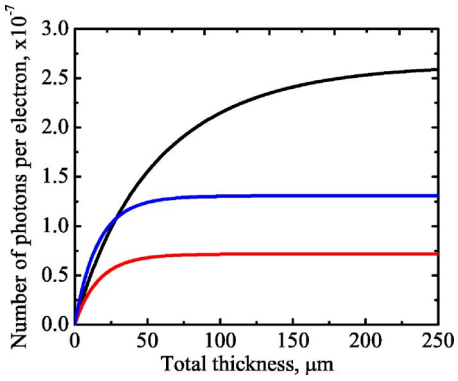

FIG. 3. (Color online) Transition radiation photon output per electron within [19.50/20.5] keV range vs the total thickness of Mo–Ag, Mo–Tl, and Mo–Pb (upper to lower curves, respectively) nanostructures with the period $l=0.2232$ μm. Electron energy is 30 MeV.

V. BREMSSTRAHLUNG AS A NOISE

At high electron and photon energies there is another major radiation process competing with TR: it is bremsstrahlung.[19] In the soft x-ray domain bremsstrahlung is significantly weaker than TR,[5,6] whereas for hard x rays it should be taken into account. As we show below, spatial filtering must be used for efficient detection of TR generated by 30 MeV electrons traversing a Mo–Ag nanostructure. In this section we study the angular distribution of both TR and BS. BS differential efficiency can be calculated in the Born approximation with screening taken into account using, e.g., the Thomas-Fermi model.[19] Including the photoabsorption into consideration, bremsstrahlung efficiency can be calculated as

$$\frac{dN_{\rm br}}{d\omega d\Omega} = \left.\frac{dN_1}{d\omega d\Omega}\right|_{\rm Ag} \frac{1-\exp(-\mu_{\rm Ag}L)}{\mu_{\rm Ag}L} + \left.\frac{dN_1}{d\omega d\Omega}\right|_{\rm Mo} \frac{1-\exp(-\mu_{\rm Mo}L)}{\mu_{\rm Mo}L}\exp(-\mu_{\rm Ag}L), \tag{24}$$

where

$$\frac{dN_1}{d\omega d\Omega} = 4\alpha Z^2 \frac{r_e^2\gamma^2 N_0 L}{2\pi\omega}\frac{4}{(x^2+1)^4} \times\left[(x^4+1)\log\frac{111(x^2+1)}{Z^{1/3}} - (x^2-1)^2\right], \tag{25}$$

$\gamma=E_0/mc^2$, $E_0=30$ MeV, μ is the photoabsorption coefficient, $x=\gamma\theta$, N_0 is the number density of material, and $L=lM/2$ is the half-width of the whole nanostructure. In Eq. (24) $dN_1/d\omega d\Omega$ should be calculated separately for Ag and Mo using Eq. (25). Figure 4 shows differential efficiency of TR and BS for 750-period Mo–Ag nanostructures in the photon energy range around the *K*-shell photoabsorption edge of Mo. One can see that the peak of TR radiation efficiency is about four times higher than the efficiency of BS radiation.

VI. DETECTORS AND MEASUREMENT ARRANGEMENT

In practice, the TR can be detected through a pinhole (see, e.g., Ref. 6), opening a small solid angle around the TR peak. Figure 5 shows angular distribution of differential efficiency of BS and TR at the TR peak energy (≈20 keV) for 750- and 250-period Mo–Ag structures. Let us consider the 250-period nanostructure and calculate the diameter of a circular pinhole suitable for experimental observation of TR. The diameter, corresponding to the half-width of the TR radiation peak would be $d=R\delta\theta_{\rm TR}$, where $\delta_{\rm TR}\approx6.1\times10^{-5}$ rad (see Fig. 5) and R is the distance from the Mo–Ag structure to the pinhole. For instance, when $R=200$ cm, the pinhole diameter $d\approx0.012$ cm.

Since bremsstrahlung radiation is quite strong in the hard x ray and its bandwidth is much broader than that of TR, the

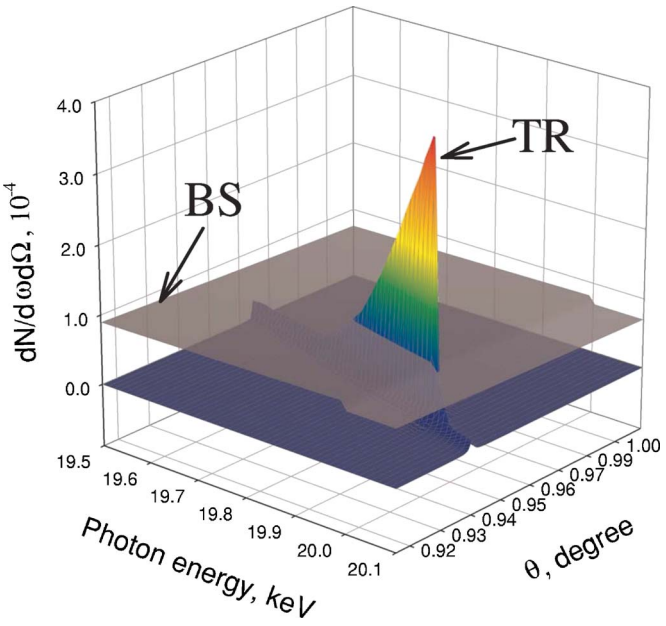

FIG. 4. (Color online) Bremsstrahlung and TR radiation efficiency in number of photons per 1 eV per steradian per electron for 750-period Mo–Ag nanostructure.

choice of x-ray detector also requires special attention. To estimate the level of BS noise, let us calculate the number of BS photons passing through the pinhole registered by the detector. The most suitable for energy range under the study are Si and CdTe detectors. We chose Amptek XR-100CR-Si-500 μm and XR-100T-CdTE-1 mm detectors and calculate the number of registered BS photons in accordance with the

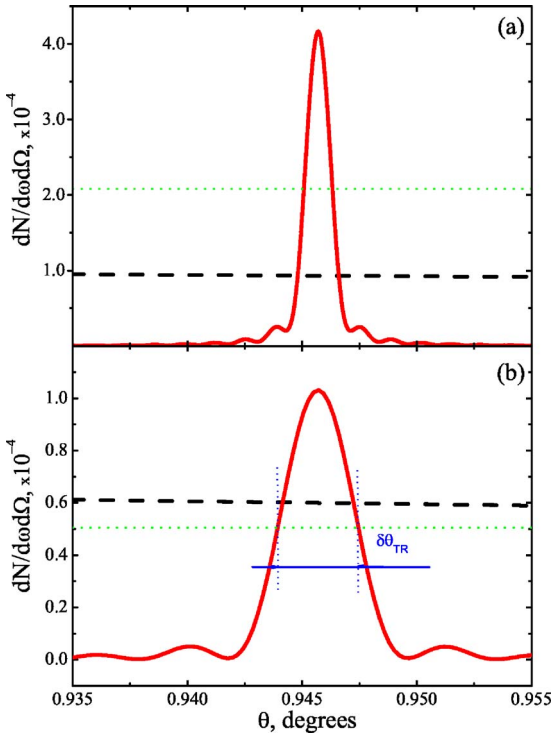

FIG. 5. (Color online) Bremsstrahlung (dashed) and TR (solid) radiation efficiency at $E_{ph}=20$ keV for 750- (a) and 250-period (b) Mo–Ag nanostructure. The dotted line corresponds to one-half of the TR peak value.

detector efficiencies[20] using the following scheme. Below 5 MeV the detection efficiency $\mathcal{E}$ of detectors is known, so that the number of detected photons is

$$\frac{dN_{\text{det}}}{d\Omega} = \int_{1\ \text{keV}}^{5\ \text{MeV}} \frac{dN_{\text{br}}}{d\omega d\Omega} \mathcal{E}(\omega) d\omega. \tag{26}$$

From 5 to 30 MeV the main mechanism contributing to the detection events is pair production:[21]

$$\frac{dN_{\text{det}}}{d\Omega} = N_0 d_D \int_{>5\ \text{MeV}} \frac{dN_{\text{br}}}{d\omega d\Omega} \sigma_{\text{pair}}(\omega) d\omega, \tag{27}$$

where

$$\sigma_{\text{pair}}(\omega) = r_e^2 Z^2 \alpha \left[\frac{28}{9} \log \frac{2\hbar\omega}{mc^2} - \frac{218}{27} \right], \tag{28}$$

d_D is the detector thickness (500 μm and 1 mm for Si and CdTe detectors, respectively), and N_0 and Z are number density and atomic number of detector material (Si or CdTe). The total number of registered BS photons is the sum of the two contributions given by Eqs. (26) and (27). For the pinhole of the diameter $d=0.012$ cm (as discussed above) placed at the angle of TR maximum ($\theta_{\text{TR}} \approx 0.9457°$) the detectors would register the following numbers of BS photons per electron passing through the pinhole: 1.62×10^{-9} (XR-100CR-Si) and 7.89×10^{-9} (XR-100T-CdTe). Thus, competing with the TR bremsstrahlung can be reduced sufficiently enough to detect the TR signal with a good margin.

VII. COHERENCY AND PRECISION TOLERANCE OF MULTILAYER STRUCTURE

Unavoidable defects and manufacturing inaccuracies (e.g., width fluctuation of the layers) in periodic structures lead to inhibition of coherent summation of TR from each period. Intensity of a signal resulted from ideally coherent summation at the exact resonant angle, $X=0$, is proportional to M^2 [see Eq. (14)], whereas in the opposite case of the fully incoherent structure the expected intensity is $\sim M$ [similar to the integration over all the modes; see Eq. (20)]. The theory of randomization-induced inhibition of coherency of multielement arrays, whereby the spacings between adjacent elements randomly deviated from the desired periodicity l_0 has been developed in Ref. 22. It has been shown that regardless of the specific statistical distribution of random width deviation in the structure, the resulting coherency is described with high accuracy by Gaussian distribution. The total gain, or the factor M^2 in Eq. (14), should now be replaced by

$$\mathcal{E}_M M, \tag{29}$$

where $1 \leqslant \mathcal{E}_M \leqslant M$ with $\mathcal{E}_M$ being a coherent enhancement.

Following Ref. 22, we introduce a normalized standard deviation σ_0 of the spacing from the designed spacing l_0 between two adjacent periods of the structure with

$$\sigma_0 = \frac{\sigma_l}{l_0}, \tag{30}$$

where σ_l is a standard deviation, and define the randomiza-

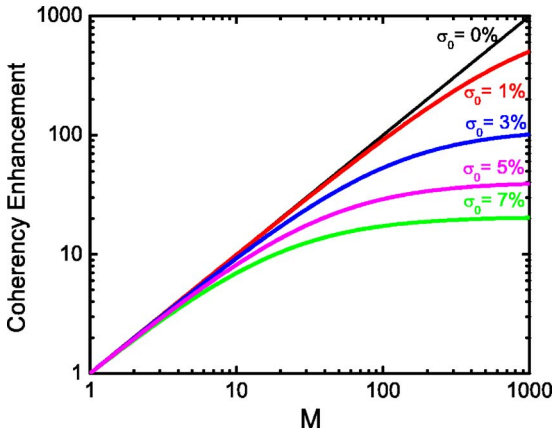

FIG. 6. (Color online) Coherency enhancement $\mathcal{E}_M$ vs the number of periods in the nanostructure for various standard deviations σ_0 [$\sigma_0=0$ corresponds to fully coherent (ideally periodic) structure].

tion parameter r and the inverse to it, *coherency range*, M_{coh}, as

$$r=(\pi\sigma_0)^2 \text{ and } M_{\mathrm{coh}}=\frac{1}{r}. \tag{31}$$

At the angle of exact resonance, $X=0$, the following relationship is valid:[22]

$$\mathcal{E}_M(X=0)=\frac{(M/2)\sinh(2r)-e^{-rM}\sinh(rM)}{M\sinh^2(r)}. \tag{32}$$

The behavior of $\mathcal{E}_M$ as function of M for various standard deviations σ_0 is depicted in Fig. 6. Assuming at least some coherence, i.e., $r\ll 1$ or $M_{\mathrm{coh}}\gg 1$, and the exact solution (32) can be reduced to a simpler formula:

$$\mathcal{E}_M(X=0)=M_{\mathrm{coh}}\left[1-\frac{e^{-\zeta}\sinh\zeta}{\zeta}\right], \quad \zeta=\frac{M}{M_{\mathrm{coh}}}, \tag{33}$$

which indicates that even when the ideal coherence is lost because of $M\gg M_{\mathrm{coh}}$, we still have $\mathcal{E}_M\approx M_{\mathrm{coh}}\gg 1$, i.e., a substantial enhancement over the case of fully random structure. Equation (33) shows that when $\zeta=1$ or $M=M_{\mathrm{coh}}$, the system exhibits only ~50% loss of coherency compared to the ideal case, thus still providing for the orders of magnitude enhancement over the fully randomized case.

It was also shown in Ref. 22 that both (32) and (33) can be approximated within better than 5% by much simpler heuristic formula, which is intuitively transparent and could be useful for practical applications in the entire range of parameters M and M_{coh}:

$$\mathcal{E}_M\approx\frac{MM_{\mathrm{coh}}}{M+M_{\mathrm{coh}}-1}=\frac{M}{(M-1)r+1}. \tag{34}$$

Let us calculate the coherency enhancement and coherency length for the Mo-based nanostructures studied above. For 10 MeV electron beam we have $l\approx 27$ nm. Assuming $\sigma_l=2.7$ Å tolerance in the period thickness, one has the standard relative deviation $\sigma_0=1\%$ and the coherency range $M_{\mathrm{coh}}\sim 10^3$, so with the total number of periods $M\sim 10^2$, one has a gain, $\mathcal{E}_M M$, only 7% below the ideally coherent gain $M^2=10^4$. With $M\sim 10^3$, one has the total gain ~50% of the fully coherent $M^2=10^6$. With the electron energy of 30 MeV, $M=750$, and for $\sigma_l=2.23$ nm and $\sigma_l=6.69$ nm one has about 60% and 14% of the fully coherent gain, respectively. Using Eq. (34) one can also calculate manufacturing precision tolerance for the multilayer nanostructure period allowing to have specific coherency gain. For example, for the 750-period nanostructure one should have $\sigma_l\lesssim 1$ nm in order to keep the TR intensity within 10% of its maximum (fully coherent) signal.

VIII. CONCLUSION

We have proposed to use the resonant transition radiation of metal-metal multilayer nanostructures in the vicinity of photoabsorption edge of constituent materials as a narrow-line source of hard x rays. Detailed analysis revealed that for hard x rays the optimal spacer-radiator pair of materials comprising the nanostructure should have the spacer, as a rule, with its atomic number larger than those of the radiator in order to eliminate the dielectric constant contrast at the far wings of the radiation line. We have applied the proposed criterion to select candidates on creation of efficient hard x-ray radiation source. For a model pair, Mo (radiator) and Ag (spacer), we have calculated the TR radiation efficiency, which shows a narrow-line near the photoabsorption edge of Mo of about 1% width. One of the most important factors in attaining an efficient source of resonant transition radiation based on atomic absorption edges becomes filtering out the Bremsstrahlung radiation. We demonstrate that for Mo–Ag couple with E-beam of 30 MeV the TR line can be well resolved when both spatial and spectral filtering is used.

ACKNOWLEDGMENT

This work is supported by AFOSR.

[1] E. Rubenstein *et al.*, Proc. SPIE **314**, 42 (1981).
[2] E. Rubenstein *et al.*, *Synchrotron Radiation in the Biosciences*, edited by B. Chance *et al.* (Oxford University Press, New York, 1994), p. 639.
[3] W. Sharf, *Biomedical Particle Accelerators* (APS, New York, 1994), Chap. 6.
[4] R. H. Huebner, *X-ray and Inner-shell Processes*, edited by T. A. Carlson, M. O. Krause, and S. T. Manson (APS, New York, 1990), pp. 161–169.
[5] A. E. Kaplan, C. T. Law, and P. L. Shkolnikov, Phys. Rev. E **52**, 6795 (1995).
[6] K. Yamada, T. Hosokawa, and H. Takenaka, Phys. Rev. A **59**, 3673 (1999).
[7] B. Lastdrager, A. Tip, and J. Verhoeven, Phys. Rev. E **61**, 5767 (1999).
[8] M. J. Moran, B. A. Dahling, P. J. Ebert, M. A. Piestrup, B. L. Berman, and J. O. Kephart, Phys. Rev. Lett. **57**, 1223 (1986).
[9] M. Karcaaltincaba and W. D. Foley, J. Comput. Assist. Tomogr. **26**, 875 (2002).
[10] The physics of resonant anomalous x-ray dispersion and scattering (with the index of refraction being part of it) has been developed in great detail in the context of crystallography, starting from A. H. Compton and S. K. Allison, *X-ray in Theory and Experiment* (Van Nostrand, New York, 1935); the excellent recent collection of articles can be found in *Resonant Anomalous X-ray Scattering: Theory and Application*, edited by G. Materlik, C. J. Sparks, and K. Fisher (North-Holland, New York, 1994). In particular, the detailed review of experimental data and earlier work are found in the papers by B. Lengeler *ibid.*, p. 35; R. L. Blake, J. C. Davis, D. E. Graessle, T. H. Burbine, and E. M. Gullikson, *ibid.*, p. 79; and D. H. Templeton, *ibid.*, p. 1. See also http://www-cxro.lbl.gov/optical_constants/
[11] V. L. Ginzburg and I. M. Frank, Zh. Eksp. Teor. Fiz. **16**, 15 (1946).
[12] G. M. Garibyan, Zh. Eksp. Teor. Fiz. **60**, 39 (1971).
[13] M. L. Ter-Mikaelian, *High Energy Electromagnetic Processes in Con-*

densed Media (Wiley Interscience, New York, 1972).
[14]M. A. Piestrup, P. F. Finman, A. N. Chu, T. W. Barbee, R. H. Pantell, R. A. Gearhart, and F. R. Buskirk, IEEE J. Quantum Electron. **19**, 1771 (1983).
[15]B. L. Henke, E. M. Gullikson, and J. C. Davis, At. Data Nucl. Data Tables **54**, 181 (1993).
[16]B. Rossi, *High-Energy Particles* (Prentice-Hall, Englewood Cliffs, NJ, 1961).
[17]For our calculations we have chosen the E-beam of 30 MeV because one of the best candidates for our future proof-of-principle experiment is Linac at Brookhaven Accelerator Test Facility, which has operating energy above 25 MeV. It must be noted, however, that for many reasons (design, accelerator accessibility, technology, bremsstrahlung noise, etc.), it is actually preferable to have lower E-beam energies, near 10 MeV.
[18]F. E. Merrill, C. L. Morris, K. Folkman, F. Harmon, A. Hunt, and B. King, Proceedings of the Particle Accelerator Conference, 2005, p. 1715.
[19]L. I. Shiff, Phys. Rev. **83**, 252 (1951).
[20]See web site http://amptek.com
[21]M. S. Longair, *High Energy Astrophysics* (Cambrige University Press, Cambridge, 1992), Vol. 1.
[22]A. E. Kaplan and S. G. Zykov, J. Opt. Soc. Am. B **22**, 547 (2005).